INTERNATIONAL JOURNAL of Industrial Education and Technology

PRE-SEISMIC IONOSPHERIC TOTAL ELECTRON CONTENT ANOMALIES ASSOCIATED WITH THE JUNE 28, 2023, EARTHQUAKE IN THAILAND

Chollada Pansong[1], Sontaya Ruttanaburee[2], Wisuit Sunthonkanokpong[3], and Prasert Kenpankho[3]*

chollada_p@rmutt.ac.th[1], sontaya512@gmail.com[2], wisuit.su@kmitl.ac.th[3], and prasert.ke@kmitl.ac.th[3]*

[1]Rajamangala University of Technology Thanyaburi, Pathum Thani 12110 Thailand
[2]Earthquake Observation Division, Thai Meteorological Department, Bangkok 10260 Thailand
[3]*King Mongkut's Institute of Technology Ladkrabang, Bangkok 10520 Thailand

*Corresponding author E-mail: prasert.ke@kmitl.ac.th

Received: September 19, 2025 Revised: October 31, 2025 Accepted: November 26, 2025

Citation reference:
Pansong, C., Ruttanaburee, S., Sunthonkanokpong, W., & Kenpankho, P. (2025). Pre-seismic ionospheric total electron content anomalies associated with the June 28, 2023, earthquake in Thailand. **International Journal of Industrial Education and Technology, 7** (2), 38 - 57.

ABSTRACT

This study investigated ionospheric Total Electron Content (TEC) anomalies as potential precursors to a moderate earthquake magnitude of 4.5 that occurred in Phai Lom, Bang Krathum District, Phitsanulok Province, Northern Thailand, on June 28, 2023 (Universal Time, UT). High-resolution GPS data from the UTHG GNSS station were analyzed at 1-second intervals over 15 days (June 21–July 5, 2023) using the ±2σ statistical boundary method to detect abnormal variations in TEC. The analysis revealed a pronounced TEC enhancement of approximately 2.61 TECU on June 23, five days before the earthquake, followed by a significant depletion on the day of the event. These variations exceeded the Upper and Lower statistical limits (UB and LB), indicating statistically significant deviations from the expected median trend. A moderate geomagnetic storm (Dst = –57 nT) was recorded on June 25; however, correlation analysis (r = –0.507) indicated only a moderate negative relationship between geomagnetic activity and TEC variations. During the earthquake period, the Dst index remained above –30 nT, signifying geomagnetically quiet conditions. To validate the findings, global TEC data obtained from the GNSS-TEC database displayed consistent temporal trends, confirming that the anomalies were not site-specific. Moreover, analysis of the Rate of TEC Index (ROTI) revealed short-term irregularities on June 23 and June 28 UT, further supporting the presence of ionospheric disturbances related to the seismic event. Overall, these results align with previous studies and emphasize the potential of GNSS-based ionospheric monitoring and correlation

analysis as reliable tools for short-term earthquake forecasting, particularly in low-latitude regions such as Thailand.

Keywords: Total electron content, Earthquake, Global navigation satellite system, Rate of TEC Index, GPS

I. INTRODUCTION

Earthquakes are natural phenomena caused by the sudden release of energy due to movement within the Earth's crust. They can occur unpredictably at any time and place, with intensities ranging from imperceptible tremors to catastrophic events that inflict severe damage to lives and property. Although Thailand is not located directly on a major tectonic plate boundary, the Department of Meteorology, Thailand, has reported the existence of 16 active fault zones within the country (Thai Meteorological Department: TMD, 2017). Historical records indicate that Thailand frequently experiences ground-level seismic shaking induced by domestic fault movements and by large-scale earthquakes originating in neighboring countries, such as Myanmar, Laos, and Indonesia, as well as the Andaman Sea. One of the most catastrophic events was the undersea earthquake in the Andaman Sea on December 26, 2004, with a moment magnitude of 9.1–9.3, which triggered a massive tsunami. This disaster claimed the lives of over 5,000 individuals in Thailand and more than 200,000 globally (TMD, 2017; United States Geological Survey: USGS, 2004). On June 28, 2023 (17:17:56, UT), an earthquake with a magnitude of MLv 4.5 at a depth of 5 kilometers (km) occurred at the epicenter near Ban Phai Lom, Bang Krathum, Phitsanulok (TMD, 2023). The cause of this earthquake was attributed to the movement of a hidden fault beneath the surface. This observation aligns with data from the USGS, which revealed the presence of many fault lines beneath the sediment layers near the Phitsanulok Basin. Interestingly, this fault line is distinct from the 16 main active fault line groups and has released unprecedented seismic energy over the past 100 years. This event was the most intense earthquake recorded in Phitsanulok over the past nine years of seismic monitoring. Despite being a relatively shallow earthquake, its strong shaking was widely felt by the general population in provinces such as Phitsanulok, Phichit, Kamphaeng Phet, Phetchabun, Nakhon Sawan, and Loei (TMD, 2023).

Despite advances in seismology, the precise prediction of earthquakes in terms of time, location, and magnitude remains unresolved. In response, we explored alternative approaches for detecting pre-seismic signals. One promising avenue involves using data from the Global Navigation Satellite System (GNSS), specifically the analysis of Total Electron Content (TEC) in the ionosphere. Variations in TEC are believed to be influenced by crustal stress accumulation, which can alter geomagnetic fields (Hofmann-Wellenhof et al., 1992, pp. 1–382; Pi et al., 1997, pp. 2283–2286; Skone & de Jong, 2014, pp. 1067–1071; Chernyshov et al., 2020, pp. 1–13; Pansong et al., 2025, pp. 7521–7532) and charged particle dynamics before seismic events (Murai, as cited in Xu et al., 2022, pp. 1–24; Liu et al., 2004, pp. 1585–1593; Pulinets, 2004, pp. 413–436; Xia et al., 2011, pp. 177–185; Heki, 2011, pp. 1–5; Cahyadi and Heki, 2013, pp. 1777-1787; Shah and Jin, 2015, pp. 42–49; Grawe and Makela, 2015, pp. 472–483; Sharma et al., 2017, pp. 65-74; Ulukavak and Inyurt, 2020, pp. 123–130; Kiyani et al., 2020, pp. 1-8; Nishioka et al., 2021, pp. 1-12; Guo et al., 2022, pp. 1-17; Sharma

et al., 2022, pp. 1–11; Nayak et al., 2024, pp. 1–21; Semlali et al., 2025, pp. 7589–7609). TEC variability arises from a complex interplay of factors that can be broadly categorized into five categories. First, space weather conditions, including solar radiation (EUV, X-rays), solar wind, solar flares, and Coronal Mass Ejections (CMEs), have a substantial influence. These phenomena, along with geomagnetic indices (e.g., Kp, Dst, and AE) and ionospheric electric fields, such as the Prompt Penetration Electric Field (PPEF) and Equatorial Electrojet (EEJ), contribute to phenomena such as the Equatorial Ionization Anomaly (EIA). Second, geographical and temporal factors, including latitude, longitude, seasonal cycles, diurnal variations, and local time, affect the distribution of TEC. Third, atmospheric coupling processes, such as gravity waves and meteorological phenomena, such as typhoons, also play a role. Fourth, lithospheric sources, such as gas or electric charge release from fault zones or volcanic eruptions, can have a transient impact on ionospheric conditions. Finally, biases in satellite signals or GNSS receivers may introduce errors in TEC estimation, necessitating correction techniques to ensure data integrity.

Previous studies have established correlations between TEC anomalies and seismic events in various regions worldwide. For example, Liu et al. (2004, pp. 1585–1593) studied pre-earthquake ionospheric perturbations recorded using continuous GPS TEC measurements. Afraimovich et al. (2004, pp. 339–354) analyzed TEC variations during the Hector Mine earthquake in California. Nishioka et al. (2021, pp. 1–12) conducted a long-term statistical analysis of TEC values over 22 years (1997–2018) in Japan, estimating 100-year return period TEC values to be 150–190 TECU in Tokyo, 180–230 TECU in Kagoshima, and 120–150 TECU in Hokkaido. Several studies have demonstrated a relationship between TEC anomalies and large earthquakes. Heki (2011, pp. 1–5) observed post-seismic increases in ionospheric electron density, though in some cases, anomalies occurred before the event. Similarly, Cahyadi and Heki (2013, pp. 1777–1787) reported TEC anomalies before the 2007 Bengkulu and 2005 Nias earthquakes in Sumatra. Shah and Jin (2015, pp. 42–49) analyzed global seismic events ($Mw \geq 5.0$) from 1998 to 2014 and found significant increases in TEC five days before earthquakes of $Mw \geq 6.0$, with 95% confidence. Their results also indicated that shallow earthquakes (depth < 60 km) have a more pronounced effect on the TEC. Sharma et al. (2017, pp. 65–74) developed a TEC-based model to detect seismic precursors in the Himalayan region, accounting for confounding factors such as geomagnetic storms and solar flares. Further evidence was presented by Ulukavak and Inyurt (2020, pp. 123–130), who reported that even small earthquakes (Mw 2.0–2.5) could induce TEC anomalies due to acoustic-gravity waves, with effects observed for up to 30 days (15 days before and after the event). In Taiwan, Guo et al. (2022, pp. 1–17) observed TEC anomalies 13–20 days before major seismic events. Semlali et al. (2025, pp. 7589–7609) studied the global correlation between Swarm satellite data and M4+ earthquakes from 2014 to 2024. They found a positive anomaly in the Magnetic Field Vector Y-component (MFV-Y) and TEC that were identified one to seven days before the earthquakes analyzed. In Southeast Asia, Kumar and Singh (2017, pp. 795–801) analyzed GPS-derived TEC data from the CUSV station in Thailand and the HYDE station in India for the 2016 Tamenglong earthquake (Mw 6.7), revealing a 47% increase in TEC about three days before the event, independent of geomagnetic influences. Eshkuvatov et al. (2025) further examined GNSS-derived TEC data from the CMUM and CUSV stations in Thailand during the Mw 7.7 Myanmar earthquake and identified anomalies

3–13 days before the mainshock. In Thailand, Pansong and Kenpankho (2025, pp. 297–312) investigated 473 earthquakes (Mw ≥ 3.0) during Solar Cycle 24 using GPS-, IGS-, and IRI-based TEC data. They observed no significant TEC correlation for Mw < 5.0, but moderate negative correlations ($r \approx -0.5$) for larger events, with TEC increasing slightly before, dropping during, and returning to normal after earthquakes. Collectively, many studies confirm the TEC–earthquake coupling mechanism and highlight the potential of GNSS-based monitoring for regional precursor detection.

Although many studies have reported correlations between ionospheric TEC variations and seismic activity worldwide, research on this topic in Thailand and Southeast Asia remains limited. Given the region's complex tectonic structure and multiple active fault zones, this study utilizes GNSS-derived TEC data to analyze ionospheric variations preceding the Phitsanulok earthquake of June 28, 2023 (UT). The Rate of TEC Index (ROTI) method was applied to identify potential pre-earthquake anomalies and to assess their temporal and spatial characteristics. In addition, the relationship between TEC variations and geomagnetic storm conditions during the earthquake period was examined to minimize the influence of external factors in this analysis. The objective is to determine whether detectable TEC disturbances occurred before the event and to evaluate their potential as short-term earthquake precursors. The findings are expected to enhance understanding of lithosphere–ionosphere interactions and support the development of more effective earthquake early-warning systems in Thailand.

II. LITERATURE REVIEW

A growing body of research has demonstrated that ionospheric TEC irregularities may serve as short-term indicators of significant seismic events. Liu et al. (2004, pp. 1585–1593) identified that 80% of large earthquakes (Mw ≥ 6.0) in Taiwan between 1999 and 2002 were preceded by nighttime TEC anomalies, particularly within five days before the mainshock. Similarly, Pulinets (2004, pp. 413-436) developed theoretical models and statistical techniques to identify ionospheric signals that could be applied to earthquake forecasting and prediction. In another high-magnitude event, Xia et al. (2011, pp. 177–185) observed consistent TEC patterns in the Qinghai–Tibet region, including two enhancement phases (at 9 and 2–3 days prior) and a period of reduced TEC (3–6 days before the events), regardless of geomagnetic interference. Heki (2011, pp. 1–5) reported a positive TEC anomaly approximately 40 minutes before the 2011 Tohoku-Oki earthquake (Mw 9.0), a finding echoed in prior mega-earthquakes such as the 2010 Chile and 2004 Sumatra–Andaman events. Cahyadi and Heki (2013, pp. 1777–1787) also reported co- and pre-seismic TEC fluctuations for the 2007 Bengkulu and 2005 Nias earthquakes, although long-term precursors were not detected in every case. Shah and Jin (2015, pp. 42–49) conducted a global analysis of 1492 earthquakes (Mw ≥ 5.0) and revealed significant TEC enhancements five days in advance of shallow quakes (depth < 60 km) of Mw ≥ 6 with high statistical confidence. Grawe and Makela (2015, pp. 472–483) explored tsunami-induced ionospheric signatures from the 2010 Chile, 2011 Tohoku, and 2012 Haida Gwaii events, underlining the roles of tsunami propagation direction and line-of-sight geometry. Kumar and Singh (2017) investigated pre-seismic ionospheric anomalies associated with the 2016 Tamenglong earthquake (M 6.7) in Northeast India using GPS-derived TEC observations. TEC data were analyzed from the CUSV station in Thailand and the HYDE

station in India to examine variations before and after the earthquake. The study applied differential TEC analysis to identify ionospheric perturbations independent of geomagnetic effects and space weather influences. Results revealed significant TEC enhancements of up to 47% approximately three days before the main shock, which gradually returned to normal afterward. In the Himalayan region, Sharma et al. (2017, pp. 65–74) modeled TEC behavior using GNSS data. They emphasized the need to account for non-seismic drivers, such as solar flares and geomagnetic storms. Ulukavak and Inyurt (2020, pp. 123–130) noted that seismo-ionospheric perturbations can emerge up to 15 days before and persist for up to two weeks after earthquakes. In parallel, Kiyani et al. (2020, pp. 1–8) identified low-intensity TEC deviations up to 10 days before the 2018 Fiji earthquake (Mw 8.2), distinguishing them from the post-seismic geomagnetic anomalies. Nishioka et al. (2021, pp. 1–12) provided statistical thresholds for extreme TEC levels in Japan based on two decades of observations, supporting the interpretation of anomalous values within a broader historical context. Similarly, Guo et al. (2022, pp. 1–17) used satellite and Global Ionospheric Maps (GIM) data to detect TEC anomalies 13–20 days before earthquakes in Taiwan, even in magnetically quiet conditions, with pre-earthquake Ne enhancements noted in the days leading up to the event. In addition, Semlali et al. (2025, pp. 7589–7609) investigated the global correlation between Swarm satellite data and M4+ earthquakes from 2014 to 2024, focusing on anomalies in MFV-Y and TEC as potential seismic precursors. Using over 200,000 earthquake events and data from three Swarm satellites, they compared observed MFV-Y and TEC values with modeled expectations from the International Geomagnetic Reference Field (IGRF) and the International Reference Ionosphere (IRI) 2020 to identify anomalies using the Unbiased Root Mean Square Difference (UbRMSD). Filtering techniques were applied to mitigate solar and geomagnetic disturbances, and the data were spatially and temporally normalized. The study employed advanced statistical methods, including Confusion Matrices (CM) and Receiver Operating Characteristic (ROC) curves, to evaluate the reliability of these anomalies in predicting seismic events. The results showed that positive MFV-Y and TEC anomalies often occurred 1–7 days before earthquakes, with better detection performance for larger magnitude events (M7+). Although high alarm rates persisted owing to overlapping ionospheric noise and solar activity, the research suggests that optimized thresholds (5 nT for MFV-Y and 0.5 TECU for TEC) can enhance early warning capability. Ultimately, this study underscores the potential of combining Swarm satellite data with statistical modeling to improve short-term earthquake forecasting, while also calling for the integration of additional geophysical indicators to reduce uncertainty and increase prediction reliability. Eshkuvatov et al. (2025) analyzed GNSS-derived TEC data from the CMUM and CUSV stations in Thailand, which were located near the Mw 7.7 earthquake in Mandalay, Myanmar. Applying the LAIC model and using input parameters from the OMNIWeb database, they examined TEC variability over 31 days and detected anomalous TEC variations 3–13 days before the main shock. Their results support the viability of GNSS-TEC monitoring as a precursor indicator of seismic activity in the Southeast Asian region, thereby providing concrete evidence that TEC-earthquake coupling can be studied using Thai station data. Additionally, Pansong and Kenpankho (2025, pp. 297–312) investigated the relationship between TEC anomalies in the ionosphere and earthquake events in Thailand during Solar Cycle 24 (2007–2020).

The research aimed to identify possible ionospheric precursors associated with moderate-to-large earthquakes by analyzing variations in TEC obtained from three sources: GPS TEC derived from 15 GNSS stations across Thailand, IGS TEC from the GIM, and IRI TEC from the International Reference Ionosphere model. A total of 473 earthquake events with magnitudes of 3.0 Mw or greater were analyzed, based on data from the Thai Meteorological Department. The study area was divided into four regions, southern and Andaman, western, northern, and northeastern Thailand, to assess spatial differences in TEC behavior. Correlation analyses were performed between TEC anomalies, earthquake magnitudes, and geomagnetic activity measured by the Kp index. The results revealed that earthquakes with magnitudes below 5.0 Mw showed no significant correlation with TEC variations. However, for events with magnitudes equal to or greater than 5.0 Mw, a moderate negative correlation was found between earthquake magnitude and TEC anomalies, with correlation coefficients of –0.495, –0.501, and –0.303 for GPS TEC, IGS TEC, and IRI TEC, respectively. Typically, TEC values increased slightly approximately three to five days before an earthquake, then decreased sharply on the day of the event, and gradually returned to normal levels within three to five days afterward. Additionally, a positive correlation ($r = 0.611$) was observed between geomagnetic storm activity (Kp index) and large earthquakes. However, no direct relationship was found between geomagnetic disturbances and short-term TEC fluctuations on earthquake days.

The present study analyzes GNSS-derived TEC data to investigate ionospheric behavior preceding the Phitsanulok earthquake of 28 June 2023 (UT). The ROTI method was employed to detect potential pre-seismic irregularities and to characterize their temporal and spatial patterns, while geomagnetic storm conditions were examined to reduce the influence of external space-weather factors. To further assess short-term ionospheric disturbances, a statistical boundary approach based on the $\pm 2\sigma$ criterion was also applied. High-resolution TEC data from the UTHG GNSS station were evaluated over a 15-day reference interval (21 June–5 July 2023), during which the mean and standard deviation for each epoch (t) were derived from TEC values recorded at the same local time across all reference days. Instantaneous TEC deviations were then calculated, and anomaly thresholds were defined as $\mu \pm 2\sigma$, with values exceeding these limits classified as potential ionospheric anomalies. By integrating the ROTI technique with the $\pm 2\sigma$ statistical boundary method, the analysis improves the reliability of distinguishing seismo-ionospheric perturbations from normal diurnal and space-weather variations. This combined approach supports the evaluation of whether detectable TEC disturbances occurred before the event and enhances the understanding of lithosphere–ionosphere coupling processes, contributing to the development of more effective earthquake early-warning systems in Thailand.

III. RESEARCH METHODOLOGY

3.1 Geomagnetic storm data

Geomagnetic storm data were incorporated in this study to evaluate the influence of geomagnetic activity on ionospheric TEC variations during the earthquake period. The hourly equatorial Dst values were obtained from the World Data Center (WDC) for Geomagnetism, Kyoto, available at https://wdc.kugi.kyoto-u.ac.jp/dst_realtime/index.html. The data were collected from June 21 to July 5, 2023, corresponding to the analysis window of this study. This information was used to examine the relationship between geomagnetic storm conditions and

TEC behavior to distinguish whether observed TEC changes were caused by geomagnetic disturbances or by seismic activity. The geomagnetic storm data are presented in Figure 1.

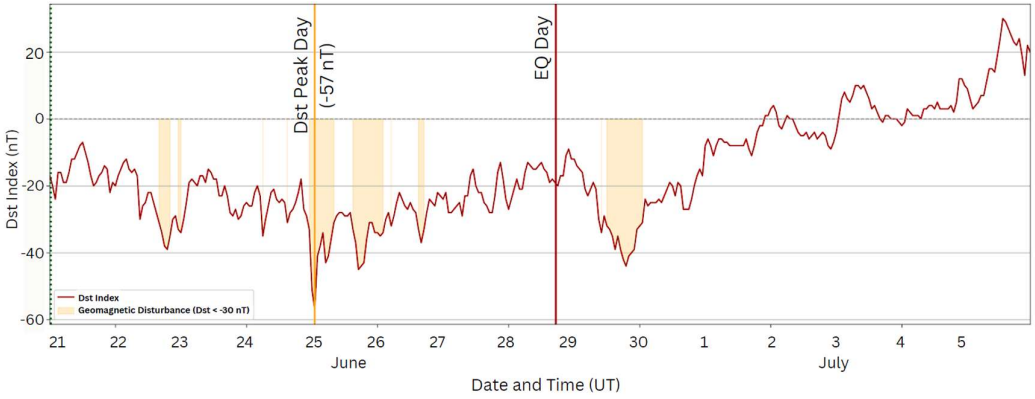

Figure 1: Geomagnetic storm with Dst index during June 21 to July 5, 2023

Figure 1 shows the temporal variation of the Dst index from June 21 to July 5, 2023 (UT). The highlighted yellow areas indicate periods of weak geomagnetic disturbances (Dst < –30 nT)

3.2 Earthquake data

On June 28, 2023 (17:17:56 UT), a moderate earthquake, recorded by the TMD as MLv 4.5, occurred in northern Thailand, located at 16.558° N and 100.368° E. Although the magnitude was relatively low compared to large-scale seismic events, the earthquake was shallow, at a depth of only 4.6 km, which increased ground shaking intensity in nearby areas. Such events are of particular interest because they may occur along previously unidentified or less-characterized fault zones. This underscores the importance of continuous monitoring and precise analysis of tectonic activity, even in regions not directly located on active plate boundaries.

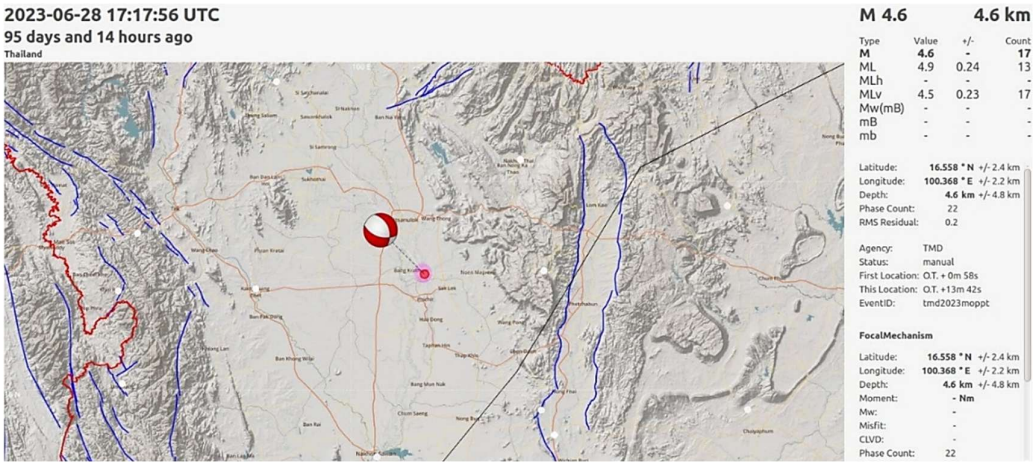

Figure 2: Seismic event map and focal mechanism of the earthquake on June 28, 2023 (UT)

Figure 2 indicates a predominantly strike-slip faulting mechanism, possibly with an oblique-slip component. The nodal planes, illustrated by the diagonally divided red and white quadrants, suggest right-lateral (dextral) motion along a southeast–northwest-trending fault. This fault orientation corresponds to the structural trend of the Phetchabun Mountain range, which lies east of the earthquake's epicenter.

3.3 The radius of the seismic epicentre area

Dobrovolsky et al. (1979, pp. 1025–1044) proposed a model to estimate the spatial extent of seismic influence by correlating earthquake magnitude with the radius of the affected area. The formulation as shown in Equation (1),

$$\rho = 10^{0.43M}, \tag{1}$$

here, the radius of the seismic epicenter area (ρ) in km is represented based on its magnitude (M).

This empirical relationship enables approximating the potential impact zone of significant seismic events by identifying regions likely influenced by precursory geophysical signals. The model further suggests that anomalies of varying physical origins, beyond ionospheric perturbations, can manifest within this calculated radius.

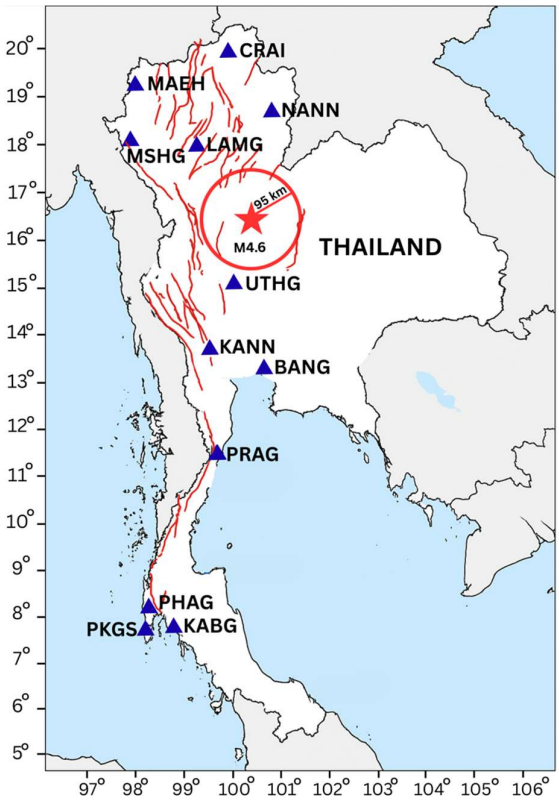

Figure 3: Epicentral location and affected radius of the June 28, 2023 (UT), earthquake in Northern Thailand

Figure 3, map of Thailand showing the epicenter (red star) of the MLv 4.5 or M 4.6 earthquake that occurred on June 28, 2023, UT, in the northern region of the country. The red circle indicates the estimated affected area with a radius of approximately 95 km, calculated using Dobrovolsky's empirical formula.GNSS stations (blue triangles) and fault lines (red lines) are also displayed to illustrate the tectonic framework and geodetic observation network relevant to this event. Earthquake parameters, including magnitude, epicentral coordinates, and depth, were obtained from the TMD GNSS station network. The data from the UTHG station in Uthai Thani Province (15.353° N, 100.009° E, elevation 27.991 m), the nearest station to the epicenter, were used as the primary reference for this study.

3.4 TEC estimation methodology using dual-frequency GPS observations

In this study, GPS-based TEC data were analyzed over 15 days, comprising seven days before and seven days after the seismic event. The TEC values (1 TECU = 10^{16} electrons/m²) were extracted from observation files in the Receiver Independent Exchange (RINEX) format, version 2.11. The slant TEC (STEC) was initially computed and then converted to Vertical TEC (VTEC) using a standard mapping function. The calculations were performed according to the procedure specified in Equations (2), (3), (4), and (5).

3.4.1 STEC

STEC was computed from carrier-phase observations at the L_1 and L_2 GPS frequencies, as outlined in prior studies (Ma & Maruyama, 2003, pp. 2083–2093; Kenpankho et al., 2011, pp. 365–370). These signals operate at frequencies of 1575.42 MHz (f_1) and 1227.60 MHz (f_2), corresponding to wavelengths of approximately 0.1902 m (λ_1) and 0.2442 m (λ_2), respectively. The relationship incorporates an ionospheric constant k of 80.62 m³/s².

$$STEC_L = \frac{2(f_1 f_2)^2}{k\left(f_1^2 - f_2^2\right)}[(L_1\lambda_1 - L_2\lambda_2) - (b_s + b_r)] \quad (2)$$

3.4.2 VTEC

VTEC was derived by converting STEC into a vertical equivalent under the assumption of a thin-shell ionospheric model. The transformation is expressed as follows:

$$STEC = \frac{VTEC}{\cos\chi}, \quad (3)$$

where χ denotes the zenith angle at the Ionospheric Piercing Point (IPP). The VTEC was further refined using an obliquity factor.

The χ is determined from the satellite elevation angle α using the following relation:

$$\chi = \arcsin\left(\frac{R_E \cos\alpha}{R_E + h}\right), \quad (4)$$

here, R_E represents the Earth's mean equatorial radius (6,378.134 km), and h denotes the height of the ionospheric shell (450 km) (Ma & Maruyama, 2003, pp. 2083–2093; Kenpankho et al., 2011, pp. 365–370). The elevation angles for estimating GPS TEC is 10 degrees to obtain VTEC with instrumental biases, as shown in Equation (5):

$$VTEC = (STEC - b_s - b_r) \times \cos \chi, \tag{5}$$

where b_s and b_r represent the satellite and receiver biases, respectively.

The estimated satellite and receiver biases were refined to improve accuracy. Based on the GPS Earth Observation Network (GEONET), an extensive GPS receiver network in Japan, Ma and Maruyama (2003, pp. 2083–2093) reported that satellite bias values typically range from 0.307 ns. For receiver bias estimation under quiet geomagnetic conditions, Kenpankho et al. (2021, p. 2157) recommended the use of the Lagrange interpolation method, with a receiver bias value of –6.25 ns.

3.5 Statistical boundary method for TEC anomaly detection

Additionally, statistical techniques were employed to define the boundary limits of TEC using the formula $\mu \pm 2\sigma$, following Ullah et al. (2025, p. 5). To further investigate the short-term TEC anomalies. To identify ionospheric anomalies, a statistical boundary method based on the ±2σ criterion was applied. High-resolution TEC data from the UTHG GNSS station were analyzed over a 15-day reference period (June 21–July 5, 2023). For each epoch (t), the mean (μ) and standard deviation (σ) of TEC were computed from the same local time across all 15 days. The instantaneous anomaly was then determined as:

$$\Delta TEC(t) = TEC_{obs}(t) - \mu(t) \tag{6}$$

The UB and LB statistical limits were defined as:

$$UB(t) = \mu(t) + 2\sigma(t), \quad LB(t) = \mu(t) - 2\sigma(t) \tag{7}$$

A deviation beyond ±2σ was classified as an anomalous TEC variation, representing approximately a 95% confidence level under quasi-Gaussian distribution assumptions. This approach enables the detection of significant departures from normal ionospheric behavior.

3.6 ROTI

The ROTI is calculated as the standard deviation of the Rate of TEC (ROT) over a specific time window, expressed in TECU/min (Pi et al., 1997, pp. 2283–2286):

$$ROTI = \sqrt{\langle ROT^2 \rangle - \langle ROT \rangle^2} \tag{6}$$

The ROT represents the first-order difference of consecutive TEC values normalized by the time interval Δt (in minutes). TEC values are given in TECU. ROTI values were computed using a 5-minute sliding window to represent short-term ionospheric irregularities.

$$ROT_i = \frac{TEC_i - TEC_{i-1}}{\Delta t} \quad (7)$$

3.7 Global TEC

To validate the accuracy and consistency of the calculated TEC values, a comparison was made with Global TEC data. The global TEC maps were obtained from the GNSS TEC database, accessible via the following link: https://stdb2.isee.nagoya- u.ac.jp/GPS/GPS-TEC/GLOBAL/AMAP/index.html#2023. This comparison aimed to verify whether the computed TEC values aligned with global trends and exhibited similar temporal and spatial patterns.

IV. RESULTS

4.1 Relationship between geomagnetic storm intensity and TEC anomalies

Table 1 presents the daily correlation coefficients (r) (Mukaka, 2012, pp. 69–71) between the Dst index and TEC anomalies to assess the influence of geomagnetic conditions on ionospheric variations during the study period as shown in Table 1.

Table 1: Daily correlation coefficients between geomagnetic activity (Dst index) and TEC anomalies from June 21 to July 5, 2023

Date (UT)	Correlation coefficients (r)	Interpretation	Note
2023-06-21	0.3559	Low, positive correlation	
2023-06-22	−0.3590	Low, negative correlation	
2023-06-23	−0.2059	Negligible correlation	Five days before EQ
2023-06-24	−0.0350	Negligible correlation	
2023-06-25	−0.5070	Moderate, negative correlation	Peak Dst day
2023-06-26	−0.0044	Negligible correlation	
2023-06-27	−0.0838	Negligible correlation	
2023-06-28	0.0833	Negligible correlation	EQ day
2023-06-29	−0.0590	Negligible correlation	
2023-06-30	−0.3638	Low, negative correlation	
2023-07-01	0.1066	Negligible correlation	
2023-07-02	−0.4094	Low, negative correlation	
2023-07-03	−0.8087	High, negative correlation	
2023-07-04	−0.0332	Negligible correlation	
2023-07-05	0.3903	Low, positive correlation	

Most days exhibited negligible correlations, suggesting that geomagnetic activity had minimal impact on TEC fluctuations. A moderate negative correlation (r = –0.507) was observed on June 25, corresponding to the peak Dst disturbance day, while on the earthquake day (June 28), the correlation was negligible (r = 0.0833) (Mukaka, 2012, pp. 69–71). These results indicate that the ionospheric TEC variations near the time of the earthquake were unlikely to be dominated by geomagnetic storm effects.

4.2 TEC anomalies

This study aimed to investigate the TEC anomalies preceding the MLv 4.5 earthquake that occurred in Thailand on June 28, 2023. By analyzing 1-second-interval TEC data from June 21 to July 5, 2023, and applying statistical boundary-detection methods, we identified potential ionospheric precursors that deviated significantly from normal diurnal variations. The figure below illustrates these anomalies and highlights their temporal relationships with the earthquake events.

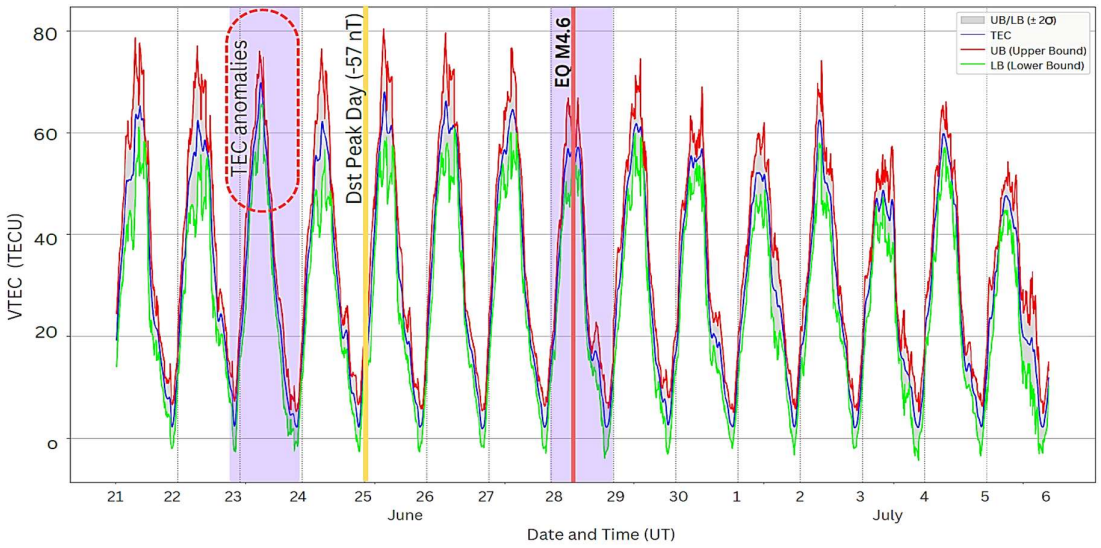

Figure 3: TEC anomalies associated with the MLv 4.5 earthquake on June 28, 2023

The time series of TEC at 1-second intervals from the UTHG station was analyzed to identify potential ionospheric precursors, with ΔTEC defined as the difference between the observed TEC and the 15-day mean TEC. Figure 3 presents the TEC variations observed from June 21 to July 5, 2023 (UT), showing the observed TEC (blue), UB (red), and LB (green). The shaded purple regions indicate significant TEC anomalies that exceeded the established statistical limits (UB and LB), most notably on June 23, 2023, approximately five days before the earthquake. An anomalous increase of about 2.61 TECU above the 15-day mean was recorded on June 23, followed by a marked decrease in TEC on the day of the earthquake (June 28, 17:17:56 UT). Thereafter, the TEC gradually returned to normal levels within four to five days. This sequence of enhancement, depletion, and recovery suggests the presence of a short-term ionospheric disturbance potentially associated with the seismic event, rather than regular ionospheric variability. The observed patterns support the hypothesis that pre-seismic TEC anomalies may serve as ionospheric precursors to moderate earthquakes in low-latitude regions such as Thailand.

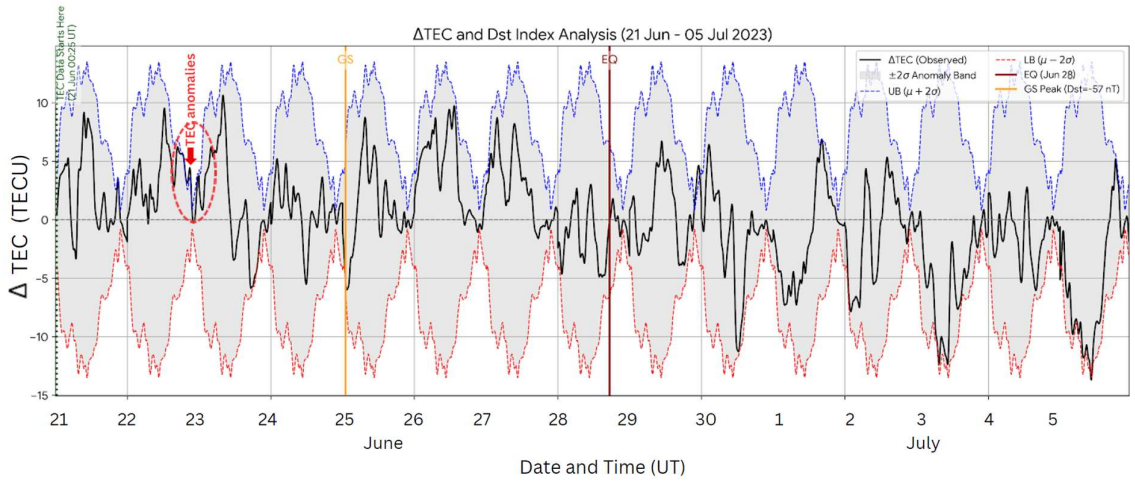

Figure 4: Time series of TEC variations and Dst index from June 21 to July 5, 2023

Figure 4 (upper panel) shows the temporal variation in ΔTEC from June 21 to July 5, 2023. The black line represents observed ΔTEC values, with the gray band indicating the normal range (±2σ). Vertical lines mark the geomagnetic storm peak (GS peak, June 25; Dst = –57 nT) and the earthquake day (EQ, June 28; MLv 4.5). The lower panel displays the hourly Dst index. Periods with Dst < –30 nT (orange zones) indicate geomagnetic disturbances, notably the drop on June 25. On the day of the earthquake, the Dst index remained stable, indicating quiet geomagnetic conditions during the event. Overall, the ΔTEC plot shows fluctuations near the ±2σ threshold approximately three to five days before the earthquake, while the Dst index remained within non-disturbed levels. This suggests that the TEC anomalies observed before the event were unlikely to be influenced by geomagnetic activity and may instead be associated with pre-seismic ionospheric perturbations.

4.3 ROTI variations

The ionosphere is sensitive to perturbations from both terrestrial and space weather influences and often exhibits detectable variations in TEC before large earthquakes. Among the key indicators of such disturbances are sudden enhancements in VTEC, fluctuations in STEC, and abrupt changes in ROTI, which reflect small-scale plasma irregularities. This study focuses on two critical dates, June 23 and June 28, 2023(UT), surrounding an MLv 4.5 earthquake. TEC parameters were extracted from the GNSS observations at the UTHG station to identify potential ionospheric signatures.

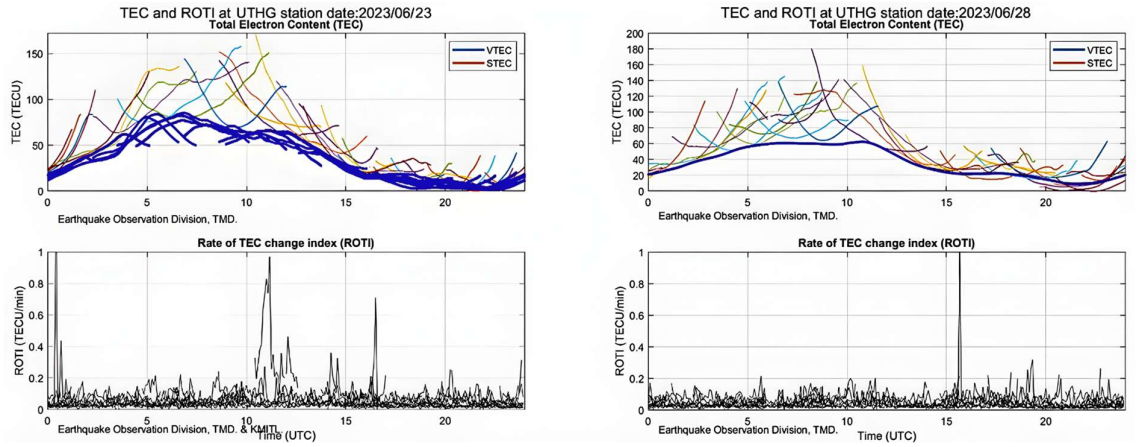

Figure 5: Daily variations of VTEC, STEC, and ROTI at the UTHG station on June 23 and June 28, 2023 (UT)

Figure 5 presents the daily variations of VTEC, STEC, and ROTI at the UTHG station on two representative days, June 23 (left) and June 28 (right), 2023. The upper panels show VTEC and STEC trends throughout the day, highlighting enhanced ionospheric activity on June 23 and a localized TEC reduction on June 28. The lower panels illustrate the ROTI values, derived at one-minute intervals to capture short-term ionospheric fluctuations. On June 23, variations in ROTI were observed between 10:00 and 16:00 UT, lasting for several hours. In contrast, on June 28, a sharp and short-lived ROTI spike occurred around 16:00 UT, closely coinciding with the earthquake time (17:17:56 UT). This spike, lasting only a few minutes, was detected under quiet geomagnetic conditions (Dst > –30 nT) and was absent during the geomagnetic storm on June 25 (Dst ≈ –57 nT). ROTI was calculated using a 5-minute sliding window (units: TECU/min). Since EIA-related scintillation typically persists for tens of minutes to hours after sunset, the brief and localized nature of the June 28 ROTI anomaly, combined with the absence of widespread regional disturbances, suggests that it was unlikely to result from routine EIA or space-weather effects. Instead, this transient feature likely reflects a localized ionospheric disturbance potentially associated with the seismic event. Both days were analyzed using the same GNSS data-processing approach. The comparison between June 23 and June 28 was intended to emphasize differences in the temporal behavior of VTEC rather than to perform a direct numerical comparison, ensuring that the observed distinctions represent genuine ionospheric variability rather than methodological bias.

4.4 Global TEC anomalies

Global TEC data were incorporated as a reference to validate the reliability of TEC values obtained from the ground-based UTHG station. This comparison ensured the consistency and accuracy of locally derived TEC, confirming that the observed variations reflected genuine ionospheric behavior rather than instrumental or processing errors. The study utilized global ionospheric TEC maps derived from GNSS-TEC observations to assess the spatiotemporal variability of TEC across Southeast Asia, with a particular focus on Thailand. The analysis covered the period from June 21 to July 5, 2023 (UT), encompassing the MLv 4.5 earthquake that occurred in northern Thailand on June 28. In Figure 6, a visual inspection of the daily

global TEC maps revealed elevated TEC over Thailand on June 23, followed by a noticeable decrease on June 28, coinciding with the earthquake. These patterns suggest the presence of possible ionospheric anomalies preceding the seismic event. The global TEC dataset was primarily used to identify large-scale ionospheric trends and to verify that regional TEC variations derived from the UTHG station were consistent with broader ionospheric behavior across the region. The purpose of this comparison was not to conduct a direct quantitative analysis but to confirm that the TEC anomalies observed over Thailand aligned with global ionospheric conditions reported by established international databases.

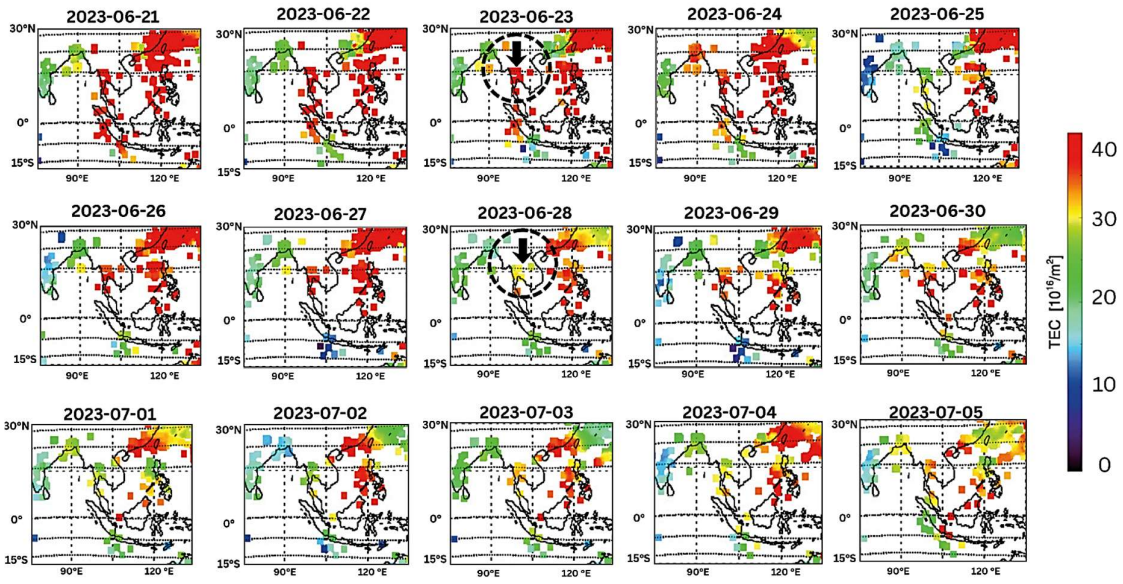

Figure 6: Global TEC maps over Thailand from June 21 to July 5, 2023

The maps in Figure 6 illustrate the spatial distribution of ionospheric TEC over Southeast Asia, with a particular focus on Thailand, outlined by a dashed black line. On June 23, five days before the MLv 4.5 earthquake, a distinct enhancement in TEC was observed over the region of interest, deviating noticeably from adjacent days. Conversely, on June 28, the day of the earthquake, a localized depletion in TEC was observed over northern Thailand, coinciding with the epicenter of the seismic event. The black circle marks the approximate earthquake location, while the black arrows indicate the regions exhibiting significant TEC variations. These anomalies suggest possible ionospheric responses linked to lithospheric processes preceding the seismic event. The TEC levels are color-coded, with higher values represented in red and lower values in blue, enabling clear visual comparison of ionospheric conditions throughout the 15-day study period.

V. CONCLUSION AND DISCUSSION

The findings of this study support the evidence that ionospheric TEC anomalies can serve as short-term precursors to seismic events. A distinct TEC enhancement of approximately 2.61 TECU was detected on June 23, 2023, five days before the MLv 4.5 earthquake in Northern Thailand on June 28, 2023, followed by a marked depletion on the day of the event. These fluctuations exceeded the ±2σ statistical boundaries, indicating statistically significant deviations from the mean trend and suggesting a possible seismo-ionospheric coupling. Complementary analyses further reinforce these findings. The ROTI results revealed a brief and localized fluctuation around 16:00–17:00 UT on the earthquake day, closely coinciding with the seismic occurrence, while geomagnetic activity remained quiet (Dst > −30 nT). In addition, the global TEC maps showed a consistent spatial pattern, with elevated TEC over Thailand on June 23 and an apparent depletion on June 28. Overall, the consistency between the local and global observations indicates that the detected ionospheric anomalies are unlikely to have resulted from regular geomagnetic or solar effects. Instead, they may reflect localized ionospheric perturbations potentially linked to pre-seismic lithospheric processes. These results highlight the potential of GNSS-based ionospheric monitoring as a valuable tool for short-term earthquake forecasting in low-latitude regions such as Thailand.

This fluctuation pattern is reminiscent of the results reported by Xia et al. (2011, pp. 177–185), who identified two phases of TEC increase occurring approximately 9 and 2–3 days before seismic events and a subsequent decline 3–6 days prior, all of which were found to be independent of geomagnetic disturbances. Similarly, Heki (2011, pp. 1–5) identified a distinct positive TEC anomaly roughly 40 minutes before the 2011 Tohoku-Oki earthquake (Mw 9.0), findings that mirror observations from the 2010 Chile and 2004 Sumatra–Andaman earthquakes. Cahyadi and Heki (2013, pp. 1777–1787) also reported both co-seismic and pre-seismic TEC anomalies for the 2007 Bengkulu and 2005 Nias earthquakes, though longer-term precursors were not consistently evident. On a broader scale, Shah and Jin (2015, pp. 42–49) conducted a global analysis of 1,492 seismic events (Mw ≥ 5.0), revealing that TEC values often rose significantly within five days preceding shallow earthquakes (depth < 60 km) with magnitudes Mw ≥ 6.0. In addition, Grawe and Makela (2015, pp. 472–483) explored ionospheric responses triggered by tsunamis following the 2010 Chile, 2011 Tohoku, and 2012 Haida Gwaii earthquakes, highlighting the impact of propagation direction and satellite geometry. In a study focused on the Himalayan region, Sharma et al. (2017, pp. 65–74) modeled TEC behavior using GNSS data. They emphasized the importance of mitigating the effects of solar and geomagnetic influences when interpreting pre-seismic anomalies. Ulukavak and Inyurt (2020, pp. 123–130) observed that disturbances in the ionosphere may persist for up to 15 days before an earthquake and for up to two weeks after. Similarly, Kiyani et al. (2020, pp. 1–8) reported mild TEC fluctuations up to 10 days before the 2018 Fiji earthquake (Mw 8.2), which could be distinguished from the post-seismic geomagnetic signals. Nishioka et al. (2021, pp. 1–12) contributed by defining statistical thresholds for abnormal TEC behavior based on two decades of GNSS observations in Japan, aiding in the reliable detection of unusual patterns. Guo et al. (2022, pp. 1–17) found consistent increases in TEC in Taiwan 13 to 20 days before earthquakes, even during periods of low geomagnetic activity. Recently, Semlali et al. (2025, pp. 7589–7609) analyzed more than 200,000 seismic events globally using satellite observations from Swarm A, B,

and C. Their analysis incorporated UbRMSD, CM, and ROC methods to identify anomalies in TEC and MFV-Y. Their results revealed that these anomalies commonly emerged one to seven days before earthquakes, especially those with Mw ≥ 7.0, although the presence of background ionospheric noise continues to present detection challenges. Collectively, these studies, along with our findings, underscore the potential of TEC anomalies as reliable short-term precursors to seismic activity. However, interpreting such anomalies must be carefully contextualized, accounting for geomagnetic, solar, and atmospheric influences, to minimize false positives and improve forecasting reliability.

ACKNOWLEDGMENT

We gratefully acknowledge the Earthquake Observation Division (EOD) of the Thai Meteorological Department (TMD) for providing the GNSS receiver infrastructure and access to raw RINEX files and seismic data across Thailand. We also appreciate the Institute for Space Earth Environmental Research (ISEE), Nagoya University, Japan, for supplying the global TEC datasets utilized in this study. We would like to thank the World Data Center (WDC) for Geomagnetism, Kyoto, Japan, for sharing the Dst index data.

REFERENCES

Afraimovich, E. L., Astafieva, E. I., Gokhberg, M. B., Lapshin, V. M., Permyakova, V. E., Steblov, G. M., & Shalimov, S. L. (2004). Variations of the total electron content in the ionosphere from GPS data recorded during the Hector Mine earthquake of October 16, 1999, California. *Russian Journal of Earth Sciences*, *6*(5), 339–354. https://doi.org/10.2205/2004ES000155.

Cahyadi, M. N., & Heki, K. (2013). Ionospheric disturbances of the 2007 Bengkulu and the 2005 Nias earthquakes, Sumatra, observed with a regional GPS network. *Journal of Geophysical Research: Space Physics*, *118*(4), 1777–1787. https://doi.org/10.1002/jgra.50208.

Chernyshov, A. A., Miloch, W. J., Jin, Y., & Zakharov, V. I. (2020). Relationship between TEC jumps and auroral substorm in the high-latitude ionosphere. *Scientific Reports, 10*(6363), 1–13. https://doi.org/10.1038/s41598-020-63422-9.

Dobrovolsky, I. P., Zubkov, S. I., & Miachkin, V. I. (1979). Estimation of the size of earthquake preparation zones. *Pure and Applied Geophysics, 117*, 1025–1044.] https://doi.org/10.1007/BF00876083.

Grawe, M. A., & Makela, J. J. (2015). The ionospheric responses to the 2011Tohoku, 2012 Haida Gwaii, and 2010 Chile tsunamis: Effects of tsunami orientation and observation geometry. *Earth and Space Science*, *2*(11), 472–483. https://doi.org/10.1002/2015EA000132.

Guo, Y., Zhang, X., Liu, J., Yang, M., Yang, X., Du, X., Lü, J., & Xiao, J. (2022). Seismo-ionospheric effects prior to two earthquakes in Taiwan detected by the China Seismo-Electromagnetic Satellite. *Atmosphere*, *13*(1523), 1–17. https://doi.org/10.3390/atmos13091523.

Heki, K. (2011). Ionospheric electron enhancement preceding the 2011 Tohoku Oki earthquake. Geophysical Research Letters, 38(17), 1–5. https://doi.org/10.1029/2011GL047908.

Eshkuvatov, H., Jin, S., Ahmedov, B., Mardonov, S., & Numonjonov, S. (2025). Pre-seismic ionospheric disturbances following the 2025 7.7 Mandalay, Burma (Myanmar) earthquake from GNSS observations. https://doi.org/10.1016/j.asr.2025.10.068.

Hofmann-Wellenhof, B., Lichtenegger, H., & Collins, J. (1992). *GPS - Global Positioning System: Theory and practice (5th edition).* Springer-Verlag.

Kenpankho, P., Watthanasangmechai, K., Supnithi, P., Tsugawa, T., & Maruyama, T. (2011). Comparison of GPS TEC measurements with IRI TEC prediction at the equatorial latitude station Chumphon, Thailand. *Earth, Planets and Space, 63*(1), 365–370. https://doi.org/10.5047/eps.2011.01.010.

Kiyani, A., Shah, M., Ahmed, A., Shah, H. H., Hameed, S., Adil, M. A., & Naqvi, N. A. (2020). Seismo ionospheric anomalies possibly associated with the 2018 Mw 8.2 Fiji earthquake detected with GNSS TEC. *Journal of Geodynamics*, *140*, 1–8. https://doi.org/10.1016/j.jog.2020.101782.

Kumar, S., & Singh, A. K. (2017). Ionospheric precursors observed in TEC due to earthquake of Tamenglong on 3 January 2016. *Current Science*, *113*(4), 795–801. http://www.jstor.org/stable/26293926.

Liu, J. Y., Chuo, Y. J., Shan, S. J., Tsai, Y. B., Chen, Y. I., Pulinets, S. A., & Yu, S. B. (2004). Pre-earthquake ionospheric anomalies registered by continuous GPS TEC measurements. *Annales Geophysicae*, *22*(5), 1585–1593. https://doi.org/10.5194/angeo-22-1585-2004.

Nayak, K., Romero-Andrade, R., Sharma, G., López-Urías, C., Trejo-Soto, M. E., & Vidal-Vega, A. I. (2024). Evaluating Ionospheric Total Electron Content (TEC) Variations as Precursors to Seismic Activity: Insights from the 2024 Noto Peninsula and Nichinan Earthquakes of Japan. *Atmosphere*, *15*(12), 1492. https://doi.org/10.3390/atmos15121492.

Nishioka, M., Saito, S., Tao, C., Shiota, D., Tsugawa, T., & Ishii, M. (2021). Statistical analysis of ionospheric total electron content (TEC): long-term estimation of extreme TEC in Japan. *Earth, Planets and Space*, *73*(1), 1–12. https://doi.org/10.1186/s40623-021-01374-8.

Ma, G., & Maruyama, T. (2003). Derivation of TEC and estimation of instrumental biases from GEONET in Japan. *Annales Geophysicae, 21*(10), 2083–2093. https://doi.org/10.5194/angeo-21-2083-2003.

Mukaka, M. M. (2012). Statistics corner: A guide to appropriate use of correlation coefficient in medical research. *Malawi Medical Journal*, *24*(3), 69–71. PMID: 23638278; PMCID: PMC3576830.

Pansong, C., Wongsak, P., Ruttanaburee, S., Pornsopin, P., & Kenpankho, P. (2025). Low latitude TEC disturbances during extreme geomagnetic storms: Insights into March and May 2024. *Advances in Space Research,76*(12), 7521–7532. https://doi.org/10.1016/j.asr.2025.03.071.

Pansong, C. & Kenpankho, P. (2025). Study on the relationship between Global Positioning System Total Electron Content anomalies and earthquake events in Thailand during Solar Cycle 24. *Earth Sciences Research Journal*, *29*(3), 297–312. https://doi.org/10.15446/esrj.v29n3.117195.

Pi, X., Mannucci, A. J., Lindqwister, U. J., & Ho, C. M. (1997). Monitoring of global ionospheric irregularities using the worldwide GPS network. *Geophysical Research Letters, 24*(18), 2283–2286. https://doi.org/10.1029/97GL02273.

Pulinets, S. (2004). Ionospheric precursors of earthquakes; recent advances in theory and practical applications. *Terrestrial Atmospheric and Oceanic Sciences*, *15*(3), 413–436. https://doi.org/10.3319/TAO.2004.15.3.413(EP).

Semlali, B.-E. B., Molina, C., Park, H., & Camps, A. (2025). Global correlation of Swarm satellite magnetic field and TEC data with M4+ earthquakes between 2014 and 2024, *Advances in Space Research*, *75*(10), 7589–7609. https://doi.org/10.1016/j.asr.2025.02.065.

Shah, M., & Jin, S. (2015). Statistical characteristics of seismo-ionospheric GPS TEC disturbances prior to global Mw ≥ 5.0 earthquakes (1998-2014). *Journal of Geodynamics*, *92*, 42–49. https://doi.org/10.1016/j.jog.2015.10.002.

Sharma, G., Champati ray, P. K., Mohanty, S., & Kannaujiya, S. (2017). Ionospheric TEC modelling for earthquakes precursors from GNSS data. *Quaternary International*, *462*, 65–74. https://doi.org/10.1016/j.quaint.2017.05.007.

Sharma, G., Romero-Andrade, R., Taloor, A. K., Ganeshan, G., Sarma, K. K., & Aggarwal, S. P. (2022). 2-D ionosphere TEC anomaly before January 28, 2020, Cuba earthquake observed from a network of GPS observations data. *Arabian Journal of Geosciences, 15*(1348). https://doi.org/10.1007/s12517-022-10605-5.

Skone, S., & de Jong, M. (2014). The impact of geomagnetic substorms on GPS receiver performance. *Earth, Planets and Space, 52*, 1067–1071. https://doi.org/10.1186/BF03352332.

Thai Meteorological Department. (2017). *Report on earthquake occurrences in Thailand and surrounding regions, 2004.* https://earthquake.tmd.go.th/report/file/seismo-report-1500882550.pdf.

Thai Meteorological Department. (2023). *Announcement from the Thai Meteorological Department, Subject: Earthquake in Phai Lom Subdistrict, Bang Krathum District, Phitsanulok Province*. https://www.tmd.go.th/warning-and-events/warning-earthquake/290620230017.

Ullah, M., Islam, F., Alarifi, N., Youssef, Y. M., Anees, Y., Ullah, I., Ahmad, M., N., & Sedeek, A. (2025). Precursory anomalies in the seismo-ionospheric-atmospheric domain associated with offshore earthquakes of magnitude greater than 7.0. *Geomatics, Natural Hazards and Risk*, *16*(1). https://doi.org/10.1080/19475705.2025.2555740.

Ulukavak, M., & Inyurt, S. (2020). Seismo-ionospheric precursors of strong sequential earthquakes in Nepal region. Acta Astronautica, 166, 123-130. https://doi.org/10.1016/j.actaastro.2019.09.033.

United States Geological Survey (USGS), (2004). *M 9.1 - 2004 Sumatra - Andaman Islands Earthquake.* https://earthquake.usgs.gov/earthquakes/eventpage/official20041226005853450_30/executive.

Xia, C.,Yang, S., Xu, G., Zhao, B., & Yu, T. (2011). Ionospheric anomalies observed by GPS TEC prior to the Qinghai-Tibet region earthquakes. *Terrestrial, Atmospheric and Oceanic sciences journal*, *22*(2), 177–185. https://doi.org/10.3319/TAO.2010.08.13.01(TibXS).

Xu, X., Chen, S., Zhang, S., & Dai, R. (2022). Analysis of potential precursory pattern at Earth surface and the above atmosphere and ionosphere preceding two Mw ≥ 7 earthquakes in Mexico in 2020-2021. *Earth and Space Science*, *9*(e2022EA002267), 1–24. https://doi.org/10.1029/2022EA002267.

The content, as well as the use of language in the article, is the responsibility of the author.